Localisation, delocalisation, and topological transitions in disordered 2D quantum walks

Jonathan M. Edge[1] and Janos K. Asboth[2]

[1] *Nordita, KTH Royal Institute of Technology and Stockholm University, Roslagstullsbacken 23 106 91 Stockholm, Sweden*
[2] *Institute for Solid State Physics and Optics, Wigner Research Centre,*
Hungarian Academy of Sciences, H-1525 Budapest P.O. Box 49, Hungary
(Dated: March 17, 2015)

We investigate time-independent disorder on several two-dimensional discrete-time quantum walks. We find numerically that, contrary to claims in the literature, random onsite phase disorder, spin-dependent or otherwise, cannot localise the Hadamard quantum walk; rather, it induces diffusive spreading of the walker. In contrast, split-step quantum walks are generically localised by phase disorder. We explain this difference by showing that the Hadamard walk is a special case of the split-step quantum walk, with parameters tuned to a critical point at a topological phase transition. We show that the topological phase transition can also be reached by introducing strong disorder in the rotation angles. We determine the critical exponent for the divergence of the localisation length at the topological phase transition, and find $\nu = 2.6$, in both cases. This places the two-dimensional split-step quantum walk in the universality class of the quantum Hall effect.

Discrete-time quantum walks[1], which we will simply refer to as quantum walks, are the quantum analogues of classical random walks. They are model systems which sit at the interface between quantum information theory and condensed matter physics. On the one hand, they form archetypical systems for studying quantum algorithms[2,3]. On the other hand, condensed matter physics has recently also shown interest in quantum walks[4–6] in particular ever since it was shown that the topological phases[7,8] can also be realised in quantum walks[9].

Condensed matter physics has a very wide scope, but one important subject of it is disorder and the associated localisation of single-particle wave functions (for a review, see Ref. 10). Thus, to understand quantum walks from the condensed matter point of view, we need to address the effect of disorder on the propagation of a quantum walker.

One of the interesting aspects of quantum walks is that in the absence of disorder the quantum walker propagates ballistically[1], thus much faster than its classical counterpart, which shows diffusive propagation. The ballistic spreading of the quantum walk is related to the quantum speed up of certain quantum algorithms, notably Grover's search algorithm[11], as the quantum walker is able to explore the search space more rapidly than its classical counterpart.

If disorder is introduced into the quantum walk system, it is expected to break the ballistic propagation of the quantum walk, analogously to the way in which disorder introduced into a solid-state system will affect electrons due to disorder scattering. This could be of relevance to the quantum information applications of quantum walks, as the quantum speed up of quantum algorithms is intimately related to ballistic propagation.

Although the effects of disorder on one-dimensional quantum walks have been extensively studied, not much is known about the two-dimensional case. For one-dimensional quantum walks it has been shown that spatial disorder can lead to exponential localisation of all energy eigenstates[12–16]. It was also found, however, that chiral symmetry can prevent localisation in one dimension[5]. To the best of our knowledge, the effects of spatial disorder in two-dimensional quantum walks and its impact on the quantum walk propagation was only studied in Ref. 17 for the Hadamard walk. In that paper it was reported that in the disordered system the wave function remains majoritatively close to the starting position, unlike in the clean case, where the amplitude of the wavefunction at the initial site decreases to zero in the long time limit. This concentration of the wave function close to its initial position (which is according to a looser terminology used as the definition of localisation, as, e.g, in Ref. 18) was attributed to Anderson localisation.

In this article we study of the effects of spatial disorder on the propagation and localisation of the Hadamard walk, and on the broader family of two-dimensional split-step walks to which it belongs. Sec. I collects the definitions of these walks, recalls their connection and their topological phases. In Sec. II we show that phase disorder localises generic split-step walks, but not the Hadamard walk: this latter shows slow diffusion (contrary to the findings of Ref. 17). In Sec. III we attribute this difference to the fact that the Hadamard walk is critical: it is a split-step walk that is tuned to a topological phase transition point. We demonstrate this phase transition and calculate the corresponding critical exponent, $\nu = 2.6$, which places the split-step walk in the quantum Hall universality class. Finally, in Sec. IV we study disorder in the angle parameters of the split-step walks. Based on the preceding section, one can expect that if the angle disorder is large enough, the split-step walk can become diffusive even with maximal phase disorder. We show that this disorder-induced delocalisation actually takes

place, and find for it the same critical exponent ν as in Sec. III. We also find that angle disorder alone leads to diffusion rather than localisation, which is probably connected to the presence of a particle-hole symmetry in this disordered quantum walk.

I. DEFINITIONS OF THE QUANTUM WALKS

A particle undergoing a quantum walk on a square lattice is represented by a time-dependent two-component wavefunction,

$$|\psi(t)\rangle = \sum_{m,n} \sum_{s=\pm 1} \psi(t)_{m,n,s} |m,n,s\rangle. \tag{1}$$

Here $m,n \in \mathbb{Z}$ give the horizontal and vertical positions on the lattice, $s \in \{+1,-1\}$ is the value of the internal state that we call spin, and $t \in \mathbb{N}$ denotes the time, which is only allowed take on discrete values. We take as initial condition a localized state, $|0,0,+1\rangle$, and obtain the time evolution by iterated applications of the time evolution operator U on the state,

$$|\psi(t)\rangle = U^t |0,0,+1\rangle. \tag{2}$$

We will consider different types of quantum walks, with the time evolution operator U consisting of a product of several shift operators and coin operators, to be defined below.

Shift operators displace the walker by one lattice site in a direction that depends on its internal state, but their action is independent of the position of the walker. We consider the quantum walk on a square lattice with the sites labelled by (m,n) and so define the following shift operators,

$$\hat{S}_x = \sum_{m,n} \sum_{s=\pm 1} |m+s,n,s\rangle \langle m,n,s|;$$
$$\hat{S}_y = \sum_{m,n} \sum_{s=\pm 1} |m,n+s,s\rangle \langle m,n,s|.$$

We use absorbing boundary conditions[19] in both the x and y directions.

Coin operators act locally on the walker, but can have position-dependent parameters. They can be written in compact form using the Pauli operators, $\sigma_z |m,n,s\rangle = s |m,n,s\rangle$; $\sigma_x |m,n,s\rangle = |m,n,-s\rangle$; $\sigma_y |m,n,s\rangle = is |m,n,-s\rangle$; and $\sigma_0 |m,n,s\rangle = |m,n,s\rangle$, for all values of m,n and s. We consider the Hadamard coin operator

$$\hat{H} = 2^{-1/2}(\sigma_x + \sigma_z). \tag{3}$$

and the spin rotation operator,

$$\hat{R}[\theta_j] = \sum_{m,n} e^{-i\theta_j^{mn}\sigma_y} |m,n\rangle \langle m,n|,$$

with θ_j^{mn} denoting the position-dependent rotation an-
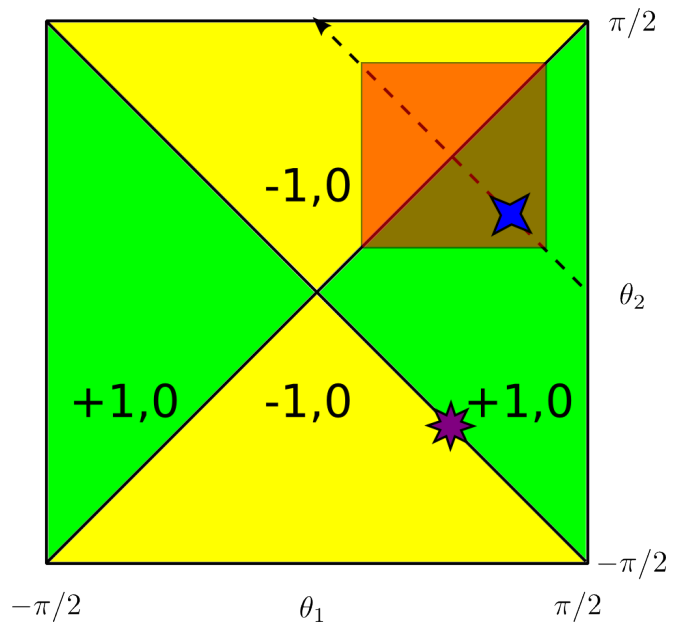

FIG. 1. (Color online) Phase diagram for the topological quantum numbers for the split-step quantum walk defined by eq. (5) without disorder[19]. As described in Ref. 19, due to the time-periodic nature of the quantum walk, two topological invariants can be defined, only one of which changes in the parameter range under consideration in this paper. The red transparent box shows the range of θ_1 and θ_2 which is accessible at the point $\theta_1 = \theta_2 = \pi/4$ for the parameters in fig. 4 and 5. The blue four-sided star shows the parameter set $\theta_1 = 0.35\pi, \theta_2 = 0.15\pi$ which is frequently used throughout this paper. The purple eight-sided star shows the parameters $\theta_1 = \pi/4, \theta_2 = -\pi/4$ at which the split-step quantum walk reduces to the Hadamard walk.

gles. The index j differentiates between rotations in one sequence of operations defining the timestep; below, the time evolution operator will contain two spin rotations, and so j will take values 1 and 2. Since $\hat{R}[\theta_j + \pi] = -\hat{R}[\theta_j]$, only angles between $-\frac{\pi}{2}$ and $\frac{\pi}{2}$ give distinct rotation operators (the minus sign is only a phase factor).

The first type of quantum walk we consider is the Hadamard walk, defined through its time evolution operator,

$$U_H = \hat{S}_y \hat{H} \hat{S}_x \hat{H}. \tag{4}$$

It thus consists of a Hadamard coin operation followed by a spin-dependent displacement in the x direction, another Hadamard coin operation rotation and a displacement in the y direction.

We also consider the split-step quantum walk[9], where the time evolution operator is defined as

$$U_s = \hat{S}_y \hat{R}[\theta_2] \hat{S}_x \hat{R}[\theta_1]. \tag{5}$$

As described in Ref. 19, for rotation angles $\theta_j^{mn} = \theta_j$ independent of position, the system has two topologi-

cal invariants: the Chern number and the quasienergy winding[20], which are determined by θ_1 and θ_2. The phase diagram for the topological invariants is reproduced in Fig. 1. The Chern number for this quantum walk is always zero, but, as we will see, the quasienergy winding plays an important role in determining the localisation properties.

The split-step quantum walk can be seen as a generalisation of the Hadamard walk. Since $H = \sigma_x e^{-i(\pi/4)\sigma_y} = e^{i(\pi/4)\sigma_y}\sigma_x$, we have

$$U_H = S_y R(-\pi/4) S_x^{-1} R(\pi/4). \qquad (6)$$

Thus the Hadamard walk is the a mirror reflected $x \leftrightarrow -x$ version of the split-step walk, with $\theta_1 = -\theta_2 = \pi/4$.

II. THE EFFECT OF PHASE DISORDER

One way to introduce discrete-time independent disorder into quantum walks, is to multiply the wavefunction at the end of each timestep by a random phase factor, which depends on position and spin value, but not on time. For this, we define the phase operators

$$\hat{P}_a[\phi] = \sum_{m,n} e^{i\phi_{mn}\sigma_a} |m,n\rangle\langle m,n|,$$

with $a = 0$ for a spin-independent, and $a = z$ for a spin-dependent phase operator. We take the phases ϕ_{mn} to have zero mean value, and distributed randomly in the interval $[-\delta\phi/2, \delta\phi/2]$. Intuitively, $\hat{P}_0$ mimics an on-site energy in a tight binding lattice model, while $\hat{P}_z$ can be understood as a disordered magnetic field. As such, these types of disorder favour localisation in non-interacting two-dimensional lattice systems[21].

A. Hadamard walk with phase disorder: Disorder-induced diffusion

To add phase disorder to the Hadamard quantum walk, Eq. (4), we define the timestep operator as

$$U_{H,a} = \hat{P}_a \hat{S}_y \hat{H} \hat{S}_x \hat{H}. \qquad (7)$$

For different values of $\delta\phi$ between 0 and 2π, and different disorder realizations, we initialise the quantum walker at the centre of a 220×220 lattice[22], and follow the time evolution for 1000 time steps.

To detect localisation, we will use two of its signatures. First, in the presence of localisation, the wave function in the long time limit should decrease exponentially as a function of the distance from the initial site,

$$\sum_{s=\pm 1} \left|\Psi(t \to \infty)^2_{m,n,s}\right| \propto e^{-2\sqrt{m^2+n^2}/\xi}. \qquad (8)$$

The localisation length $\xi \in \mathbb{R}$ of a localized wavefunction
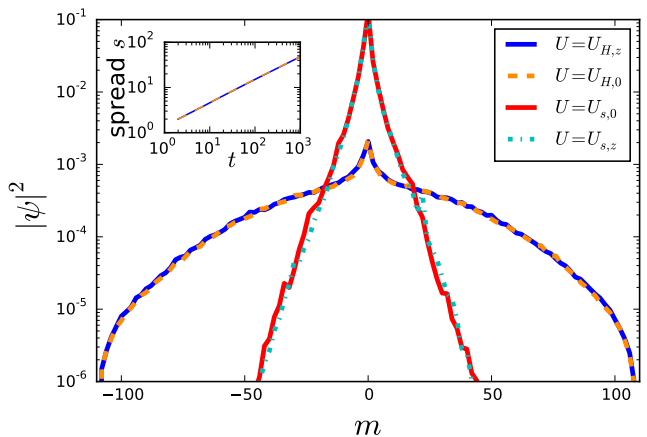

FIG. 2. (Color online) Wavefunction cross-section at $n = 0$ after 1000 time steps for a quantum walker initialised at the centre of an 220x220 lattice, averaged over 500 disorder realisations. Only even lattice sites are shown, as the wave function is zero on odd lattice sites for $t = 1000$. In total four types of quantum walks are shown: $U_{H,a}$ (Eq. (7)) and $U_{s,a}$ (Eq. (10)) with $a = 0, z$, $\delta\phi = 2\pi$. For $U_{s,a}$ we choose $\theta_1 = 0.35\pi$, $\theta_2 = 0.15\pi$ and $\delta\theta = 0.14\pi$. As we can see, $U_{H,0}$ and $U_{H,z}$ show similar types of diffusive behaviour. The inset shows the spreading of the wavefunction for $U_{H,z}$ and $U_{H,0}$ (same color coding as in the main figure), which it is roughly consistent with the diffusive $s \sim \sqrt{t}$ behaviour. In contrast, $U_{s,0}$ and $U_{s,z}$ show localising behaviour according to Eq. (8).

should be well defined (at least in the vicinity of the initial site). Second, in the localised case, the spreading $s(t)$ of the wave function, defined as

$$s^2(t) = \sum_{m,n}\sum_{s=\pm 1}(m^2 + n^2)|\Psi(t)_{m,n,s}|^2, \qquad (9)$$

should saturate, i.e., $\lim_{t\to\infty} s(t) = \text{const}$.

In the Hadamard walk with phase disorder, we find diffusive dynamics instead of localisation. In Fig. 2 we have plotted a cross-section of the probability amplitude squared of the wave function after 1000 timesteps of both the Hadamard walk with spin-dependent, and spin-independent disorder, averaged over 500 disorder realizations. We see that although the wave function is strongly peaked towards the centre, it does not decay exponentially: in both cases, it shows a Gaussian profile characteristic of diffusive behaviour[23]. The inset shows the spreading $s(t)$, which displays no sign of saturation: it is well approximated by $s(t) \propto t^{1/2}$, which again is an indication of diffusion.

Our results contradict those of Ref. 17, where localisation was found for the disordered Hadamard walk, and also go against the intuitive picture that onsite disorder induces localisation. Although it cannot, in principle, be ruled out that localisation will eventually set in, the 1000 times steps we considered give an already significantly larger timescale than the 20 time steps investigated in
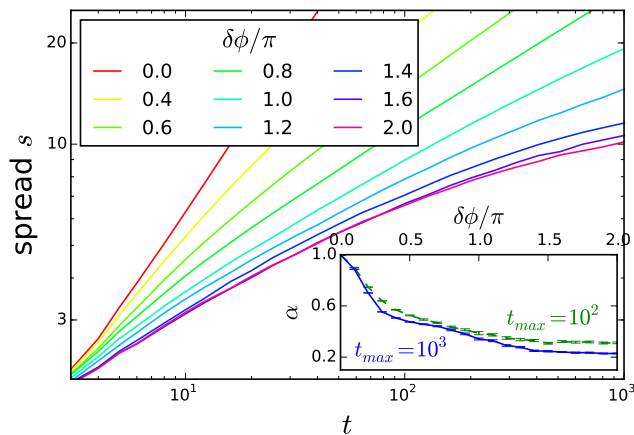
FIG. 3. (Color online) Spreading $s(t)$ of the wavefunction in the quantum walk $U_{s,0}$ of Eq. (10) as a function of time, with various amounts of phase disorder $\delta\phi$, averaged over 100 disorder realisations (log-log plot). The rotation angle parameters are set to $\theta_1 = 0.35\pi, \theta_2 = 0.15\pi$. Upon increasing the phase disorder, the walk shifts from a delocalised ($s(t) \propto t^\alpha$) to a localised ($\lim_{t\to\infty} s(t) = \mathrm{const}$) behaviour. Inset: exponent α of $s(t) \propto t^\alpha$ fitted to the curves between $t_{min} = 10$ and t_{max} (blue solid line: $t_{max} = 100$, green dashed line: $t_{max} = 1000$). For, $\delta\theta = 0$, the system behaves ballistically, with $\alpha = 1$. For larger disorder the fitted value of α decreases with time, indicating localisation.

Ref. 17. Why is there no localisation in the disordered Hadamard walk? This is one of the main questions which we will answer below.

B. Split-step walk with phase disorder: Disorder-induced localisation

To obtain a full picture of phase disorder and its effects on localisation, we now apply disorder to the generic split-step walk, which can be seen as a generalization of the Hadamard walk, cf. Eq. (6). We fix the rotation angles at $\theta_1 = 0.35\pi$ and $\theta_2 = 0.15\pi$. As seen on the phase space of the walk, Fig. 1, this set of parameters is far from the continuous lines along which the quasienergy gap closes. The time evolution operator is then given by

$$U_{s,a} = \hat{P}_a[\phi]S_yR[\theta_2]S_yR[\theta_1], \qquad (10)$$

with $a = 0$ for spin-independent, and $a = z$ for spin-dependent disorder. We remark that both types of phase disorder break the particle-hole symmetry of the system, which arose since U_s was real[9].

Our numerical results indicate that unlike the Hadamard walk, the 2-D split-step quantum walk is localised by phase disorder. As shown in Fig. 3, in the absence of phase disorder, $\delta\phi = 0$, the wave function spreads ballistically, as expected. As $\delta\phi$ is increased, however, the wave function spreads more slowly, and for large values of $\delta\phi$, it seems to saturate indicating localisa-

tion. The inset of Fig. 3 shows the localisation transition through the exponent α obtained by fitting $s(t) \propto t^\alpha$ to the numerical results over short ($10 < t < 100$, green dashed) and long[24] ($10 < t < 1000$, blue solid) times. When $\delta\phi = 0$ we observe ballistic propagation, indicated by a time-independend value of $\alpha = 1$. For increasing values of disorder α decreases and, more importantly, decreases as a function of time. This indicates that a power law fit for $s(t)$ does not provide a good fit and that the system is localising. Additional evidence for localisation is furnished by the shape of the wavefunction in the long-time limit, as shown in Fig. 2.

III. TOPOLOGICAL TRANSITION BEHIND DELOCALIZATION

The difference in the effects of phase disorder on the Hadamard walk (diffusion) and the generic split-step quantum walk (localisation), is due to the fact that the Hadamard walk is a special case of the split-step walk, tuned to a topological phase transition point. In this Section we expand on this explanation, and investigate it numerically, obtaining the critical exponents corresponding to this phase transition via single parameter scaling.

To make sure that the effect we observe is generic, we also include a small amount of disorder in the angle parameters of the split-step quantum walk. These angles θ_j^{mn} will be chosen randomly and independently for each site, from a uniform distribution in the interval $[\theta_j - \delta\theta, \theta_j + \delta\theta)$. Thus the first and second rotation have the same disorder $\delta\theta$, which we fix in this section to be $\delta\theta = 0.2\pi$.

A. Topological transition by tuning the mean rotation angles

We locate the topological phase transition, by tuning the parameters of the quantum walk: we gradually increase θ_2 from 0 to $\pi/2$ while keeping $\theta_1 + \theta_2 = \pi/2$ constant, all the while keeping maximal phase disorder, $\delta\phi = 2\pi$, and a moderate angle disorder, $\delta\theta = 0.2\pi$. This path is marked by the dashed line in Fig. 1. We characterise the localisation properties for each set of parameter values via the time-dependent diffusion coefficient,

$$D(t) = \frac{s^2(t)}{t}. \qquad (11)$$

In the long-time limit the diffusion coefficient $D(t)$ is a constant in regimes governed by diffusion (metallic or possibly critical regimes) and decreases in time in the localised regime ('non-metallic' regime). We choose this quantity because it will be a suitable starting point for the scaling analysis of the transition point.

Our results for the diffusion coefficient D for various times, as the rotation angles θ_j are tuned across topological phase transition, are shown in Fig. 4. At most values
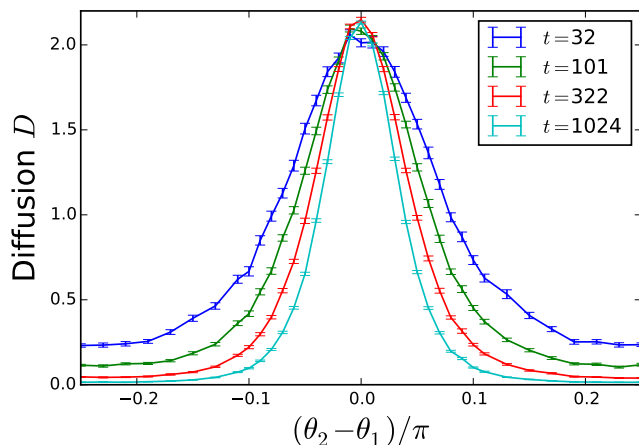
FIG. 4. (Color online) Diffusion coefficient as a function of $\theta_2 - \theta_1$ with $\theta_1 + \theta_2 = \pi/2$ for $\delta\theta = 0.2\pi$, $\delta\phi = 2\pi$, obtained by averaging over 100 disorder realisations on a 220x220 lattice.

of the angles, the calculated values of $D(t)$ decrease with time t, and we can infer that the quantum walk is localised. At the point $\theta_1 = \theta_2 = \pi/4$, however, the curves of $D(t)$ corresponding to various times overlap, and so the system is diffusive. This is a delocalisation transition.

We attribute the delocalisation at $\theta_1 = \theta_2 = \pi/4$ to the occurrence of a topological phase transition. In the absence of disorder, the quantum walk has topological invariants $(-1, 0)$, and $(+1, 0)$ at the endpoints of the path, respectively. It is thus plausible that somewhere along the path a topological phase transition has to occur. Our observations show that this transition occurs at the point $\theta_1 = \theta_2 = \pi/4$, which is also what one might expect on symmetry grounds.

Another angle from which to understand the delocalisation at $\theta_1 = \theta_2 = \pi/4$ is the following. At the interface between two domains of the quantum walk with different topological phases there are edge states[19]. If both possible topological quantum numbers occur locally with equal probability, a percolating network of edge states appears. At $\theta_1 = \theta_2 = \pi/4$ the possible local values of θ_1 and θ_2 are shown by the red transparent box in Fig. 1. This network can be thought of as a realisation of the Chalker-Coddington network model for the integer quantum Hall effect[25], tuned to the plateau transition point. At this point a non-zero conductance appears, which in this case is signalled by a diffusively spreading wavefunction.

B. Scaling analysis of the localisation-delocalisation transition

In this section we perform a scaling analysis of the transition at $\theta_1 = \theta_2 = \pi/4$, where the localisation length ξ of Eq. (8) has to diverge. We use the same approach as for the corresponding transition in the quantum anoma-

lous Hall effect[26]: we compute high accuracy data for the diffusion coefficient $D(t)$, and then we fit this data assuming power-law divergence of the localization length and single-parameter scaling. We summarize the main ideas and the results here and relegate the details to Appendix A.

The split-step quantum walk with generic values of θ_1 and θ_2 has a phase-disorder-dependent localisation length ξ, defined in Eq. (8). This quantity effectively determines how far the wave function may spread. At a topological transition the localisation length has to diverge (there is no length scale associated with diffusive, i.e., metallic propagation). We assume that this divergence happens as a power law, in analogy with the quantum Hall case[27],

$$\xi = A \left| \eta \right|^{-\nu}; \tag{12}$$

Here η is the distance from the critical point, A is a constant of proportionality and ν is the critical exponent[10]. When this transition is obtained as explained above, along the line $\theta_1 + \theta_2 = \pi/2$, the role of η is played by

$$\eta = \theta_2 - \theta_1. \tag{13}$$

Instead of measuring the localisation length ξ directly (which would require a calculation of $D(t)$ up to much larger times), we find ν by assuming single-parameter scaling of the diffusion coefficient $D(t)$ of Eq. (11). Taking finite-time corrections[23] into account, we have

$$\ln D(t) = F(t^{1/2\nu}u) + t^{-y}G(t^{1/2\nu}u); \tag{14}$$

$$u = \eta + \mathcal{O}(\eta^2). \tag{15}$$

Here the scaling functions $F(z)$, $G(z)$, and $u(z)$, as well as the exponents y and ν are to be fitted to the numerical data. The quality of the fits will provide justification for the single parameter scaling assumption.

We computed the high accuracy data for the fitting procedure by simulating the quantum walk on an 800×800 lattice for varying number of timesteps over many disorder realizations. A large number of disorder realizations was used for the runs at shorter times (4001, 4001, 2001,1001, to obtain $D(t)$ at $t = 32, 80, 203, 512$, respectively), whereas due to self averaging, fewer disorder realizations already provided enough accuracy for the runs at longer times (200 realizations for $t = 8192, 3250, 1290$). The resulting values of $D(t)$ were then fitted with the scaling Ansatz, Eq. (14), using a Taylor series expansion of the functions F, G, and u to various orders. Instead of converging to a single solution, we obtained a good fit to the data for different forms of the scaling functions, and also different values of the exponents – an example is shown in Fig. 5, lower panel. To represent our estimate of the critical exponent ν, we define an estimator function $E(\nu)$, whose integral between any two values $\nu_{\min}$ and $\nu_{\max}$ reflects our degree of confidence that $\nu_{\min} < \nu < \nu_{\max}$. The construction of this func-

FIG. 6. (Color online) Diffusion coefficient as a function of $\delta\theta$ for $\delta\phi = 2\pi$, $\theta_1 = 0.35, \theta_2 = 0.15$, obtained by averaging over 100 disorder realisations on a 220x220 lattice.
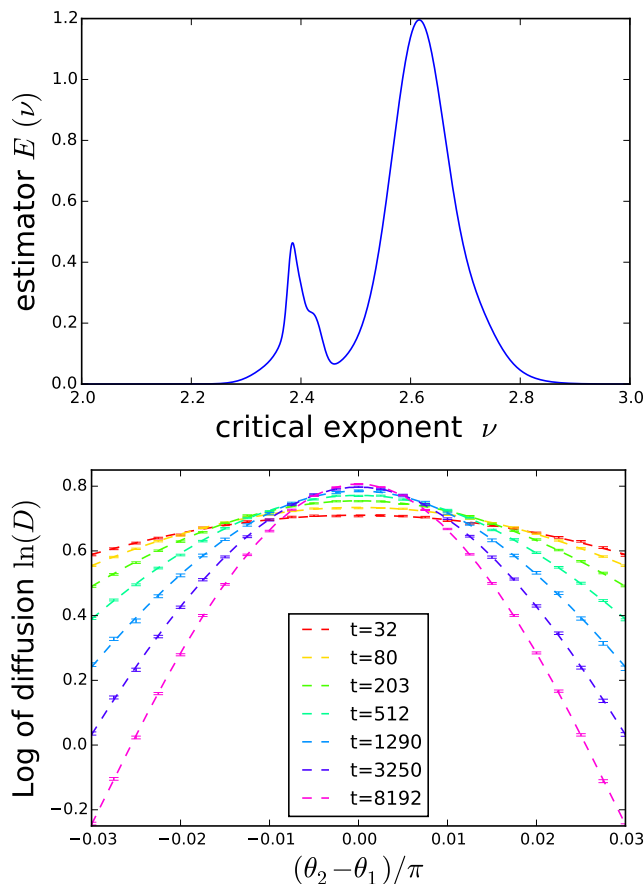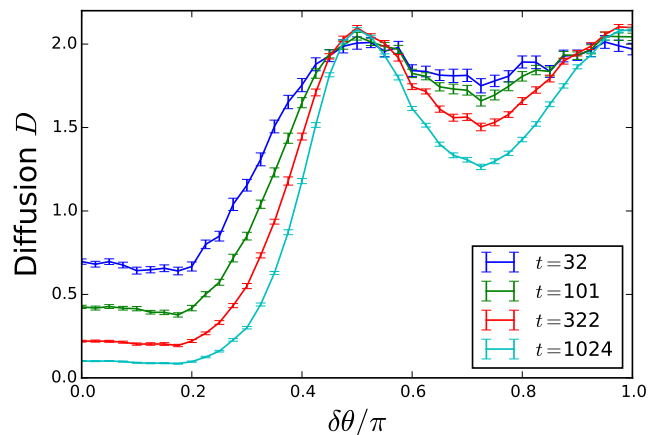
FIG. 5. (Color online) Top panel: estimator of critical exponent obtained. Rather than providing a histogram we have plotted the curve as a sum of 60 normalised Gaussians as given by eq. (A5) ($N_{max} = 60$). In the bottom panel we show an example scaling fit to the diffusion coefficient data, demonstrating that the data for different t and $\theta_2 - \theta_1$ can be fitted to a single scaling function. Here $J = 8, K = 3$ and $L = 1$ were chosen and $\nu = 2.592$ at $\xi^2/ndf = 0.94$ was obtained. The 68% confidence interval was found to be $[2.557, 2.625]$.

tion, along with the details of the fitting procedure, are explained in Appendix A.

As seen in Fig. 5, our estimator of the critical exponent ν is a bi-modal function, with a peak around $\nu_m = 2.616$ (full width at half the maximum of 0.125), and a second peak at $\nu_2 = 2.384$. The value corresponding to the larger peak, $\nu_m = 2.616$, is very close to the quantum Hall critical exponent[27] of 2.593 ± 0.003. The smaller peak is close to previous estimates of the exponent of the quantum Hall transition[10], which are now attributed to bi-stability of the fitting procedure, possibly related to finite-size effects[28]. To summarize, the transition which we observe is compatible with the integer quantum Hall transition universality class.

IV. DISORDER IN THE ROTATION ANGLES OF THE SPLIT-STEP WALK

We already introduced disorder to the rotation angles of the split-step quantum walk, although with a small value of $\delta\theta = 0.2\pi$, in the previous sections. We now examine what happens to the quantum walk as this disorder grows. We first consider a split-step quantum walk that is localised by maximal phase disorder. As we turn on the angle disorder $\delta\theta$, we will find that at special values of $\delta\theta$, the walk delocalises. We then consider a split-step walk with no phase disorder, only angle disorder. We find that, contrary to what one might expect, angle disorder does not induce localisation.

A. Competition of phase and angle disorder: Disorder-induced delocalisation

We now consider what happens if we first localise a quantum walk by phase disorder, as in section II B, and then increase the disorder in the rotation angles $\delta\theta = \delta\theta_1 = \delta\theta_2$ to π. At this maximal value, as well as at $\delta\theta = \pi/2$, all inequivalent values of the rotation angles are equally likely. According to the network model pictured described in Sec. III A, we expect a percolating network of edge states and thus expect delocalised behaviour at these values of the rotation angle disorder.

Our numerics clearly show the disorder-induced delocalisation, at both $\delta\theta = \pi/2$ and $\delta\theta = \pi$. We plot the time-dependent diffusion coefficient $D(t)$ in Fig. 6, as a function of $\delta\theta$, at fixed mean values of the rotation angles, $\theta_1 = 0.35\pi$, $\theta_2 = 0.15\pi$, and maximal phase disorder, $\delta\phi = 2\pi$. The diffusion coefficient decreases with time, indicating localised dynamics, except near the points of maximal disorder, $\delta\theta = \frac{\pi}{2}$ and π: there the system is diffusive.

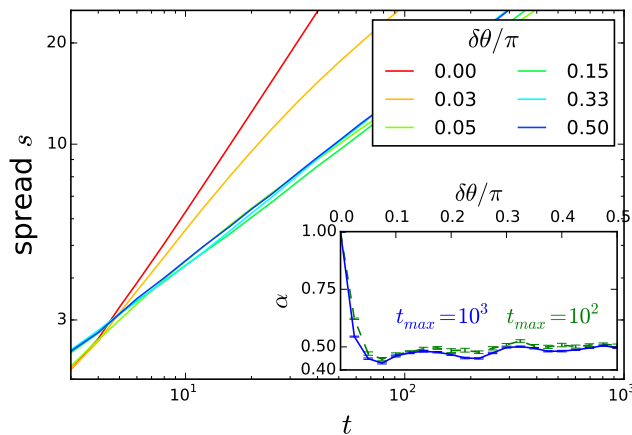We believe that the disorder-induced delocalisation we

FIG. 7. (Color online) Spread of the quantum walker averaged over 100 disorder realisations, for $\theta_1 = 0.35\pi, \theta_2 = 0.15\pi$ in the absence of phase disorder, as the angle disorder is increased from 0 to its maximal value of $\pi/2$. Just like Fig. 3 the inset shows the fitted power law exponent of $s(t) \propto t^\alpha$. For large $\delta\theta$ we obtain a time-independent $\alpha \approx \frac{1}{2}$, unlike in the case where phase disorder was present.

observe here accompanies a topological phase transition, much like in the case of Fig. 4. Indeed, for $\delta\theta < \pi/2$ the majority of sites have parameters corresponding to topological invariants of $(+1,0)$, whereas for $\pi/2 < \delta\theta < \pi$, the majority topological invariant is $(-1,0)$. It is thus plausible that at $\delta\theta = \pi/2$ a topological phase transition occurs. We performed a scaling analysis on this transition, with now the control parameter being $\eta = \delta\theta - \pi/2$. We obtained consistent results of $\nu = 2.58 \pm 0.05$, in agreement with the mode of the distribution of $\nu_m = 2.6$ shown in Fig. 5. This confirms that the exponent ν is universal: its value does not depend on the method we use to drive the system across the transition.

B. Diffusive behaviour in the presence of only rotation angle disorder

Finally we investigate the spreading of the split step quantum walk in the presence of only rotation angle disorder. We fix the mean rotation angles to $\theta_1 = 0.35\pi$ and $\theta_2 = 0.15\pi$. This choice of the mean rotation angles places the system in an insulating phase with topological invariants $(+1,0)$, as shown by the blue four-sided star in Fig. 1.

In Fig. 7 we show the result of increasing the rotation angle disorder from $\delta\theta = 0$ to $\delta\theta = 2\pi$. We observe the expected ballistic behaviour at $\delta\theta = 0$, and already for rather small values of $\delta\theta$ we see the crossover to the diffusive regime with $s \propto t^{1/2}$. Unlike in the case with phase disorder, though, we don't observe any signs of localisation here.

Although we do not have a complete explanation for this absence of localisation, we believe it is related to

the particle-hole symmetry of the system, that is not broken by rotation angle disorder. The time evolution operator has only real elements in position basis, and thus, the effective Hamiltonian possesses particle-hole symmetry represented by complex conjugation. In time-independent lattice systems, the presence of this symmetry leads to non-universal behaviour, and in some cases to diffusion instead of Anderson localisation[10].

V. SUMMARY AND CONCLUSION

To summarise, we have found that the Hadamard walk is not localised by phase disorder, while generic split-step quantum walks are. We gave an intuitive physical explanation for this difference, namely, that the Hadamard walk is a split-step walk tuned to a topological phase transition. We corroborated this picture by numerically demonstrating that this transition can be reached through angle disorder as well, at precisely the value that this explanation predicts. We determined the critical exponent for the divergence of the localisation length for both of these routes to criticality, and found $\nu = 2.6$, which places the split-step quantum walk with phase disorder in the universality class of the quantum Hall effect. We have also found that angle disorder alone does not localise the split-step quantum walk, which may be due to the fact that this disorder does not break the particle-hole symmetry of the system.

A useful next step to strengthen our interpretation of the localisation effects of disorder would be the calculation of the topological invariant of the disordered split-step walk, the quasienergy winding. Here, any of the existing approaches to the Chern number in disordered systems can be of use. One could extend the definition of the quasienergy winding[20] using noncommutative geometry[29,30], or measure the winding number of the scattering matrix[26,31,32].

Another interesting question to pursue concerns at which point (and whether) the disorder-driven delocalisation transition occurs for non-uniform disorder distributions, e.g. gaussian disorder distributions for θ_1 and θ_2 or a binary distribution (with the two sets of (θ_1, θ_2) having different topological invariants).

Our interpretation of the localization phenomena relied on qualitative similarity with disordered quantum (anomalous) Hall insulators: we even obtained the same critical exponent. However, there are also ways in which these two disordered systems differ from each other. In the quantum anomalous Hall insulator study, a disorder-induced splitting of the transition from Chern number $+1$ to -1 into two transitions was observed[26]. In the present paper, on the other hand, no such splitting of the trasition from quasienergy winding $+1$ to -1 was found. To better understand these differences, perhaps the 4-step walk[19] can help, as it can realize all possible combinations of trivial/nontrivial Chern number and quasienergy winding.

Appendix A: Details of the scaling analysis

We determine the critical exponent ν by a scaling analysis as used in Refs. 26 and 33, which will allow us to classify to which universality class this localisation transition belongs. Instead of measuring the localisation length ξ directly from the numerics, we assume single parameter scaling, and determine ξ from the diffusion coefficient $D(t)$ of Eq. (11). The scaling law for the logarithm of the diffusion coefficient in dynamical localisation[23] reads[34]

$$\ln D(t) = \tilde{F}(\xi^{-2}t). \tag{A1}$$

Here the scaling function $\tilde{F}(z)$ is some continuous, differentiable function of its argument z.

We insert the power law diverging behaviour for ξ, given by Eq. (12), into Eq. (A1), rescale the function $\tilde{F}$, and add finite-time corrections[23] to obtain

$$\ln D(t) = F(t^{1/2\nu}u) + t^{-y}G(t^{1/2\nu}u); \tag{A2}$$

$$u = \eta + \mathcal{O}(\eta^2). \tag{A3}$$

Here the function F is related to $\tilde{F}$ as

$$F(z) = \tilde{F}(z^{2\nu}/A^2), \tag{A4}$$

where A is the constant from Eq. (12). The function G takes into account finite-time corrections, with y denoting the first subleading exponent. We expand the formulae for $\ln D$ and u of Eq. (A2) in Taylor series,

$$\ln D = \sum_{j=0}^{J} f_j(t^{1/2\nu}u)^j + \sum_{k=1}^{K} t^{-y}g_k(t^{1/2\nu}u)^{k-1}$$

$$u = \eta + \sum_{l=3}^{L} u_l\eta^l.$$

Since the function $\ln D$ must be even, j may only take even values. In contrast, k and l may only take odd values, though $k = 0$ is also allowed, $k = 0$ corresponding to the absence of finite-time corrections. We choose the order of the approximation by fixing $J, K, L \in \mathbb{N}$, and then fit the Taylor coefficients f_j, g_k, u_l, and the exponents y and ν to the $D(t)$ data. This allows us to obtain an estimate for the critical exponent ν.

We fitted the numerically obtained data for $D(t)$ with 90 different functions, defined by different values of $J \in \{2\ldots10\}$, $K \in \{0,1,3\ldots9\}$, and $L \in \{1,3,5\}$. In a first approach, we systematically increased the order of the approximation, i.e., the values of J, K and L, until we obtained a reasonable goodness of fit. Unfortunately, this did not yield a uniform convergence, neither when the standard χ^2-test was used (value of χ^2 per degree of freedom (χ^2/ndf) of order 1), nor when the more sophisticated goodness of fit measure[35], Q, was used. We thus resorted to an alternative approach, as explained below.

We represent our results for the critical exponent ν, by use of an estimator function $E(\nu)$, obtained by the following procedure. Out of the 90 different fitting functions $\mathcal{F}_i$, we reject those which gave a value of χ^2 outside of an acceptance range, $0.5 < \chi^2/ndf < 2$. For the remaining 60 functions $\mathcal{F}_i$, with critical exponents ν_i, we used the bootstrap method to evaluate the goodness of fit Q_i, and the 68% confidence interval for the critical exponent: $\nu \in [\nu_i - \sigma_i^-, \nu_i + \sigma_i^+]$. The estimator $E(\nu)$ is then defined as

$$E(\nu) = \frac{1}{N_{max}} \sum_{i=1}^{N_{max}} \sqrt{2\pi\sigma_i} \exp\left(-\frac{(\nu - \nu_i)^2}{2\sigma_i^2}\right), \tag{A5}$$

with $N_{max} = 60$, and $\sigma_i = (\sigma_i^+ + \sigma_i^-)/2$. This is the probability density of the critical exponent, if we deem all acceptable outcomes of our fitting procedure equally likely.

[1] J. Kempe, Contemporary Physics **44**, 307 (2003).
[2] N. Shenvi, J. Kempe, and K. B. Whaley, Phys. Rev. A **67**, 052307 (2003).
[3] V. Potoček, A. Gábris, T. Kiss, and I. Jex, Phys. Rev. A **79**, 012325 (2009).
[4] T. Kitagawa, E. Berg, M. Rudner, and E. Demler, Physical

Review B **82**, 235114 (2010).

[5] H. Obuse and N. Kawakami, Physical Review B **84**, 195139 (2011).

[6] J. K. Asbóth, Physical Review B **86**, 195414 (2012).

[7] M. Hasan and C. L. Kane, Reviews of Modern Physics **82**, 3045 (2010).

[8] X.-L. Qi and S.-C. Zhang, Reviews of Modern Physics **83**, 1057 (2011).

[9] T. Kitagawa, M. S. Rudner, E. Berg, and E. Demler, Physical Review A **82**, 033429 (2010).

[10] F. Evers and A. D. Mirlin, Reviews of Modern Physics **80**, 1355 (2008).

[11] L. K. Grover, Physical Review Letters **79**, 325 (1997).

[12] Y. Yin, D. E. Katsanos, and S. N. Evangelou, Physical Review A **77**, 022302 (2008).

[13] A. Schreiber, K. N. Cassemiro, V. Potoček, A. Gábris, I. Jex, and C. Silberhorn, Physical Review Letters **106**, 180403 (2011).

[14] A. Ahlbrecht, V. B. Scholz, and A. H. Werner, Journal of Mathematical Physics **52**, 102201 (2011).

[15] A. Joye, Quantum Information Processing **11**, 1251 (2012).

[16] J. Ghosh, Physical Review A **89**, 022309 (2014).

[17] J. Svozilík, R. d. León-Montiel, and J. P. Torres, Physical Review A **86**, 052327 (2012).

[18] N. Inui, Y. Konishi, and N. Konno, Physical Review A **69**, 052323 (2004).

[19] J. K. Asboth and J. M. Edge, (2014), arXiv:1411.3958.

[20] M. S. Rudner, N. H. Lindner, E. Berg, and M. Levin, Phys. Rev. X **3**, 031005 (2013).

[21] E. Abrahams, P. W. Anderson, D. C. Licciardello, and T. V. Ramakrishnan, Physical Review Letters **42**, 673 (1979).

[22] Throughout this article we choose lattice sizes large enough for the boundary to have no effect.

[23] G. Lemarié, J. Chabé, P. Szriftgiser, J. C. Garreau, B. Grémaud, and D. Delande, Physical Review A **80**, 043626 (2009).

[24] For small values of disorder the walker spreads very rapidly, such that it reaches the boundary before $t = 1000$. For these cases we have fitted α in the range $10 \leq t \leq t_{\delta\phi}$ where $t_{\delta\phi}$ is chosen to be a time before the walker has reached the boundary.

[25] J. T. Chalker and P. D. Coddington, Journal of Physics C: Solid State Physics **21**, 2665 (1988).

[26] J. P. Dahlhaus, J. M. Edge, J. Tworzydł o, and C. W. J. Beenakker, Physical Review B **84**, 115133 (2011).

[27] K. Slevin and T. Ohtsuki, Physical Review B **80**, 041304 (2009).

[28] K. Slevin and T. Ohtsuki, , 10 (2012), arXiv:1203.1384.

[29] E. Prodan, Journal of Physics A: Mathematical and Theoretical **44**, 239601 (2011).

[30] M. B. Hastings and T. A. Loring, Journal of Mathematical Physics **51**, 015214 (2010).

[31] I. C. Fulga, F. Hassler, and A. R. Akhmerov, Phys. Rev. B **85**, 165409 (2012).

[32] M. Pasek and Y. D. Chong, Phys. Rev. B **89**, 075113 (2014).

[33] J. M. Edge, J. Tworzydł o, and C. W. J. Beenakker, Physical Review Letters **109**, 135701 (2012).

[34] We choose $\ln D$ instead of D to perform scaling on, since this makes the fitting simpler, as only a lower order expansion of the fitting function is required. This follows Ref. 26.

[35] W. H. Press, S. A. Teukolsky, W. T. Vetterling, and B. P. Flannery, *Numerical recipes: The art of scientific computing* (Cambridge University Press, 2007).